available at www.sciencedirect.com
journal homepage: www.europeanurology.com

European Association of Urology

Review – Prostate Cancer

Prostate Imaging Reporting and Data System Version 2.1: 2019 Update of Prostate Imaging Reporting and Data System Version 2

Baris Turkbey[a,†,*], *Andrew B. Rosenkrantz*[b,†,*], *Masoom A. Haider*[c], *Anwar R. Padhani*[d], *Geert Villeirs*[e], *Katarzyna J. Macura*[f], *Clare M. Tempany*[g], *Peter L. Choyke*[a], *Francois Cornud*[h], *Daniel J. Margolis*[i], *Harriet C. Thoeny*[j], *Sadhna Verma*[k], *Jelle Barentsz*[l,‡], *Jeffrey C. Weinreb*[m,‡]

[a] *Molecular Imaging Program, National Cancer Institute, NIH, Bethesda, MD, USA;* [b] *Department of Radiology, NYU Langone Medical Center, New York, NY, USA;* [c] *University of Toronto, Lunenfeld-Tanenbaum Research Institute, Sinai Health System, Toronto, Canada;* [d] *Paul Strickland Scanner Centre, Mount Vernon Cancer Centre, Northwood, UK;* [e] *Department of Radiology, Ghent University Hospital, Gent, Belgium;* [f] *Department of Radiology and Radiological Science, Johns Hopkins University School of Medicine, Baltimore, MD, USA;* [g] *Department of Radiology, Brigham and Women's Hospital, Boston, MA, USA;* [h] *Department of Radiology, Hôpital Cochin, Université Paris Descartes, Paris, France;* [i] *Weill Cornell Imaging, Cornell University, New York, NY, USA;* [j] *Department of Radiology, Hôpital Cantonal de Fribourg HFR, University of Fribourg, Fribourg, Switzerland;* [k] *Department of Radiology, University of Cincinnati, College of Medicine, Cincinnati, OH, USA;* [l] *Department of Radiology and Nuclear Medicine Radboudumc, Nijmegen, The Netherlands;* [m] *Department of Radiology, Yale School of Medicine, New Haven, CT, USA*

Article info

Article history:
Accepted February 25, 2019

Associate Editor:
James Catto

Keywords:
Prostate cancer
Prostate Imaging Reporting and Data System Version 2
Prostate Imaging Reporting and Data System Version 2.1

Abstract

The Prostate Imaging Reporting and Data System version 2 (PI-RADS v2) was developed with a consensus-based process using a combination of published data, and expert observations and opinions. In the short time since its release, numerous studies have validated the value of PI-RADS v2 but, as expected, have also identified a number of ambiguities and limitations, some of which have been documented in the literature with potential solutions offered. To address these issues, the PI-RADS Steering Committee, again using a consensus-based process, has recommended several modifications to PI-RADS v2, maintaining the framework of assigning scores to individual sequences and using these scores to derive an overall assessment category. This updated version, described in this article, is termed PI-RADS v2.1. It is anticipated that the adoption of these PI-RADS v2.1 modifications will improve inter-reader variability and simplify PI-RADS assessment of prostate magnetic resonance imaging even further. Research on the value and limitations on all components of PI-RADS v2.1 is strongly encouraged.

† Drs. Turkbey and Rosenkrantz contributed equally to this manuscript.
‡ Drs. Barentsz and Weinreb share the senior authorship of this manuscript.
* Corresponding authors. 10 Center Drive, Building 10, Room B3B85, Bethesda MD 20892, USA. Tel. +1 2407606112 (B. Turkbey). Department of Radiology, NYU Langone Health, 660 First Avenue, New York, NY 10016, USA. Tel. +1 212 263 0232 (A.B. Rosenkrantz).
E-mail address: turkbeyi@mail.nih.gov (B. Turkbey), Andrew.Rosenkrantz@nyulangone.org (A.B. Rosenkrantz).

https://doi.org/10.1016/j.eururo.2019.02.033
0302-2838/Published by Elsevier B.V. on behalf of European Association of Urology.

1. Introduction

Multiparametric magnetic resonance imaging (mpMRI) is increasingly being utilized for the detection and risk stratification of clinically significant prostate cancer (csPCa) [1,2], and there are continued requirements to standardize techniques and train radiologists in its optimal application [3]. To address these requirements, the American College of Radiology, European Society of Urogenital Radiology (ESUR), and AdMeTech Foundation convened an international expert panel to develop the Prostate Imaging Reporting and Data System version 2 (PI-RADS v2) [4]. PI-RADS v2 is designed to standardize image acquisition techniques and interpretation of prostate MRI, which is critical for management, communication, comparative research involving multiple institutions, and quality assurance for multicenter trials. PI-RADS v2 has received rapid and broad international acceptance among radiologists and urologists, and is widely utilized in daily practice and research [5]. Indeed, recent studies have documented the impact of PI-RADS v2 on the detection of csPCa [6–10]. To ensure that radiologists can be properly trained in PI-RADS v2, educational courses are offered by various organizations.

PI-RADS v2 was developed with a consensus-based process using a combination of published data, and expert observations and opinions. After 3 yr of development, it was released on-line (https://www.acr.org/Quality-Safety/Resources/PIRADS) in late 2014 and published in early 2016 [11,12]. Subsequently, numerous studies have validated the value of PI-RADS v2, but, as expected, they have also shown some inconsistencies and limitations. For example, interobserver agreement has only been good to moderate [13,14], and a number of specific assessment criteria have been identified, which require clarification or adjustment [15]. Furthermore, certain technical issues concerning the acquisition of mpMRI data would benefit from updating and refinement.

To address these issues, the PI-RADS Steering Committee, again using a consensus-based process, has recommended several modifications to PI-RADS v2, maintaining the framework of assigning scores to individual sequences and using these scores to derive an overall assessment category. Given the restricted scope of these updates, the updated version, described below, is termed PI-RADS v2.1.

2. Revisions in image data acquisition

Revisions in technical parameters for image acquisition of mpMRI data incorporated into PI-RADS v2.1 include the following specifications.

2.1. Technical specifications of T2-weighted acquisition

In the technical specification for PI-RADS v2, it stated that "multiplanar (axial, coronal, and sagittal) T2-weighted (T2W) images are usually obtained." Since evaluation of T2 signal intensity and morphology, including lesion encapsulation, plays important roles in PI-RADS assessment, and this evaluation can be limited by partial volume averaging when viewing in only one plane, PI-RADS v2.1 states that "T2W images should always be obtained in the axial plane (either straight axial to the patient or in an oblique axial plane matching the long axis of the prostate) and a minimum of one additional orthogonal plane (i.e., sagittal and/or coronal)."

2.2. Technical specifications of diffusion-weighted image acquisition

For the generation of apparent diffusion coefficient (ADC) maps, PI-RADS v2 advised the use of a low *b* value between 50 and 100 s/mm^2 to avoid contamination of the measured diffusion signal by "perfusion" effects. While this "perfusion contamination" seemed to be important when PI-RADS v2 was written, the use of a minimum *b* value of 50–100 s/mm^2 was found to be technically more challenging than the use of a minimum *b* value of 0 s/mm^2 for some magnetic resonance (MR) systems, and it is likely that perfusion effects do not substantively impact clinical interpretation of diffusion-weighted imaging (DWI).

Diffusion kurtosis effect occurs when using *b* values $>$1000 s/mm^2 and may impact calculation of ADC values. Hence, PI-RADS v2.1 recommends that the highest *b* value used to calculate ADC is $\leq$1000 s/mm^2 [16].

Thus, in PI-RADS v2.1, technical specification for DWI has been revised: "For ADC map calculation, it is recommended to use one low b-value set at 0–100 sec/mm^2 (preferably 50–100 sec/mm^2) and one intermediate b-va^{l}ue set at 800–1000sec/mm^2. A high b-value ($>$ = 1,400 sec/mm^2) is also mandatory and preferab^{l}y should be obtained from a separate acquisition or calculated from the low and intermediate b-value images".

2.3. Technical specifications of dynamic contrast enhanced MRI acquisition

PI-RADS v2 suggested a temporal resolution of $\leq$10 s ($<$7 s preferred). However, subsequent investigations have not shown any added diagnostic benefit from such high temporal resolution imaging [17,18], and it could potentially result in important compromises in image quality, including spatial resolution. The technical specifications have therefore been changed in PI-RADS v2.1 to advise a temporal resolution of $\leq$15 s. However, a more rapid temporal resolution may be selected if sufficient spatial resolution is maintained and overall image quality is guaranteed.

In addition, PI-RADS v2 indicated that dynamic contrast enhanced (DCE) MRI could be performed using either two-dimensional (2D) or two-dimensional (3D) acquisition. Recognizing the widespread availability of 3D DCE sequences on current systems and expert consensus that 3D acquisitions have signal-to-noise ratio (SNR) advantages compared with 2D acquisitions for DCE, this has been updated in PI-RADS v2.1 to state that "while both 2D or 3D T1 W gradient echo (GRE) sequences have been used, 3D T1 W GRE is preferred."

3. Clarifications in interpretation criteria

Modifications in interpretation criteria of mpMRI data incorporated into PI-RADS v2.1 include assessment of lesions in the central zone (CZ) and the anterior fibromuscular stroma (AFMS), evaluation of the transition zone (TZ), revision of criteria for DWI scores 2 and 3, and clarification of the distinction between positive and negative enhancement on DCE MRI.

3.1. Assessment of lesions in the CZ and AFMS

PI-RADS v2 provided assessment criteria for findings in the peripheral zone (PZ) and TZ, which together account for most csPCa cases. If there are no abnormal findings in the CZ or AFMS, it stated that the CZ and AFMS should not be reported separately. However, lesions are occasionally encountered, which appear to originate in the CZ or involve the AFMS, and warrant special consideration.

PI-RADS v2.1 modifications are as follows.

3.1.1. Central zone

The normal CZ is usually visible on T2W and ADC images as bilaterally symmetric low-signal-intensity tissue encircling the ejaculatory ducts from the prostatic base to the verumontanum [19]. It is symmetrically, mildly hyperintense on high *b*-value DWI, and it demonstrates neither early enhancement nor asymmetrically increased signal intensity on high *b*-value DWI (Fig. 1). PCa originating in the CZ is uncommon, and most of these arise in either the adjacent PZ or the adjacent TZ, and extend into the CZ. Focal early enhancement and/or asymmetry between the right and left CZs on T2W, ADC, or high *b*-value images is a finding that may indicate the presence of PCa (Fig. 2). However, asymmetry in size alone may be a normal variant, especially in the setting of benign prostatic hyperplasia (BPH) in the TZ, which may deform, displace, or cause asymmetry of the CZ.

Occasionally, the normal CZ may appear as a discrete nodule in the midline above the level of the verumontanum; a symmetric signal on ADC/DW images and/or lack of early contrast enhancement may help differentiate benign from malignant tissue.

3.1.2. Anterior fibromuscular stroma

The normal AFMS shows bilaterally symmetric shape ("crescentic") and symmetric low signal intensity (similar to that of obturator or pelvic floor muscles) on T2W, ADC, and high *b*-value DWI without early enhancement (Fig. 3). Abnormalities with increased T2W signal intensity relative to the pelvic muscles, high signal intensity on high *b*-value DWI, low signal on ADC compared with adjacent pelvis muscle signal intensity (and hence relatively lower signal on ADC than normal AFMS), asymmetric enlargement or focal mass, and early enhancement may all be helpful in detecting PCa that has extended into the AFMS (Fig. 4) [20]. Since PCa does not originate in the AFMS, when reporting a suspicious lesion in the AFMS, criteria for either the PZ or the TZ should be applied, depending on the zone from which the lesion appears most likely to be originating [21]. It is understood that the zone of origin is not always certain—an inevitable limitation of PI-RADS assessment methodology.

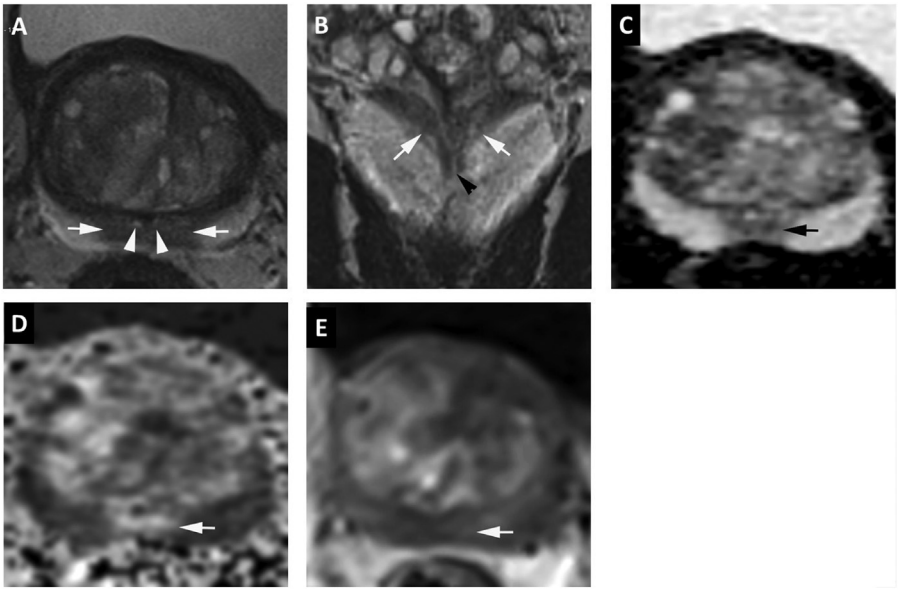

Fig. 1 – Normal central zone. (A) Axial T2-weighted image shows symmetric homogeneous hypointense signal (arrows) surrounding the ejaculatory ducts (arrowheads) at the prostate base. (B) Coronal T2-weighted image shows symmetric homogeneous hypointense signal (arrows) in a cone-shaped distribution extending from the base to the level of verumontanum (arrowhead) in the mid gland. (C) ADC map axial image shows symmetric mildly hypointense signal corresponding to (A) (arrow). (D) Diffusion-weighted image (*b* = 1400) shows symmetric mildly hyperintense signal corresponding to (A) and (B) (arrow). (E) Early dynamic contrast enhanced image shows no enhancement in the region of the central zone (arrow). T2W MRI PI-RADS = 1, DW MRI PI-RADS = 1, DCE MRI PI-RADS = negative, PI-RADS assessment category = 1. ADC = apparent diffusion coefficient; DCE = dynamic contrast enhanced; DW = diffusion weighted; MRI = magnetic resonance imaging; PI-RADS = Prostate Imaging Reporting and Data System; T2W = T2 weighted.

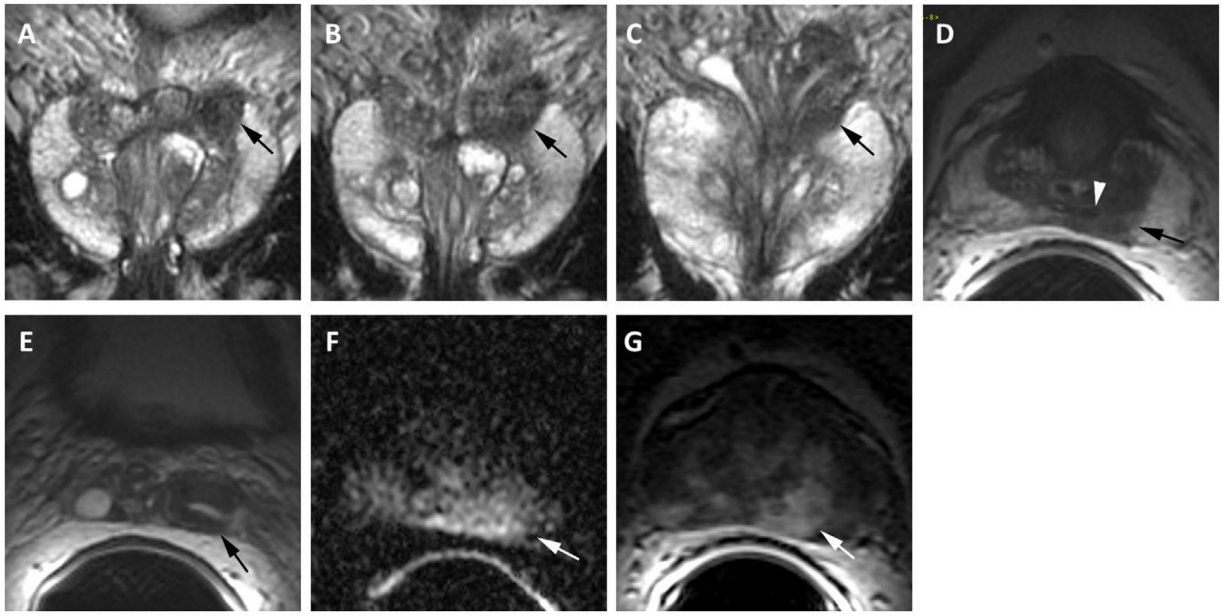

Fig. 2 – Central zone prostate cancer. MRI performed at 1.5 T with endorectal coil in a 59-yr-old man with prostate cancer (radical prostatectomy adenocarcinoma showing Gleason 4 + 3 prostate cancer in the left base with extraprostatic extension and left seminal vesicle invasion). (A–C) Coronal T2-weighted images show an asymmetric T2 moderately hypointense signal involving the left base with extension into the left seminal vesicle (arrow). (D) Axial T2-weighted image shows asymmetric T2 moderately hypointense signal (arrow) in the left central zone surrounding the left ejaculatory duct (arrowhead). (E) Axial T2-weighted image shows asymmetric thickening of the wall of the left seminal vesicle (arrow). (F) Axial diffusion-weighted image for b = 1000 s/mm^2 shows an asymmetric hyperintense signal in the left central zone. (G) Axial dynamic contrast-enhanced image shows early intense asymmetric enhancement corresponding to signal abnormalities on T2W and DWI images. T2W MRI PI-RADS = 5, DW MRI PI-RADS = 5, DCE MRI PI-RADS = positive, PI-RADS assessment category = 5. DCE = dynamic contrast enhanced; DW = diffusion weighted; DWI = diffusion-weighted imaging; MRI = magnetic resonance imaging; PI-RADS = Prostate Imaging Reporting and Data System; T2W = T2 weighted.

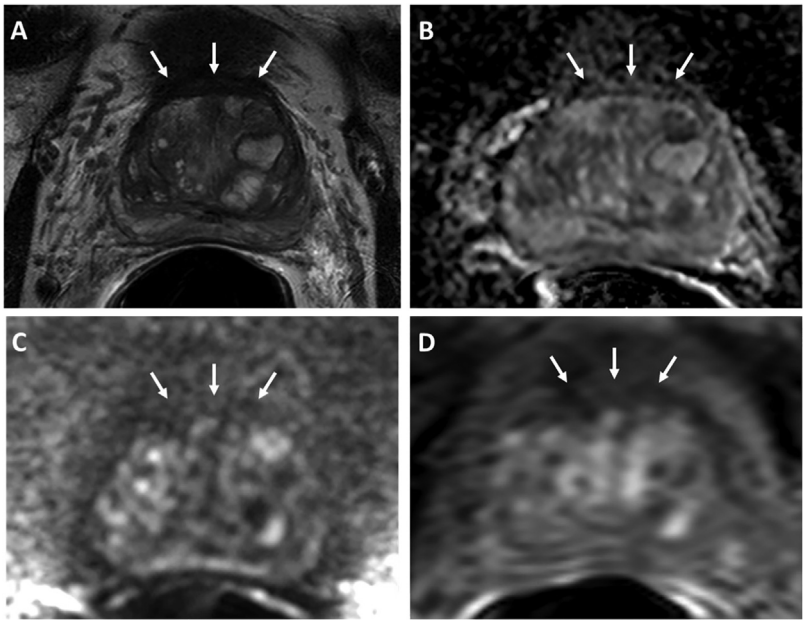

Fig. 3 – Normal anterior fibromuscular stroma (AFMS), which is composed of vertically oriented smooth muscle bundles continuous with the bladder smooth muscle and covers the anterior surface of the prostate as a nonglandular layer. (A) Axial T2-weighted image shows a symmetric markedly hypointense signal along the anterior aspect of the prostate, typical of normal AFMS (arrows). (B) ADC map axial image shows normal signal (similar to that of the background prostate) along the AFMS, which is typical of normal AFMS (arrows). (C) Diffusion-weighted image (b = 2000) shows normal hypointense signal (similar to that of the background prostate) along the AFMS (arrows). (D) Early dynamic contrast enhanced image shows lack of enhancement along the AFMS (arrows). T2W MRI PI-RADS = 1, DW MRI PI-RADS = 1, DCE MRI PI-RADS = negative, overall PI-RADS = 1. ADC = apparent diffusion coefficient; DCE = dynamic contrast enhanced; DW = diffusion weighted; MRI = magnetic resonance imaging; PI-RADS = Prostate Imaging Reporting and Data System; T2W = T2 weighted.

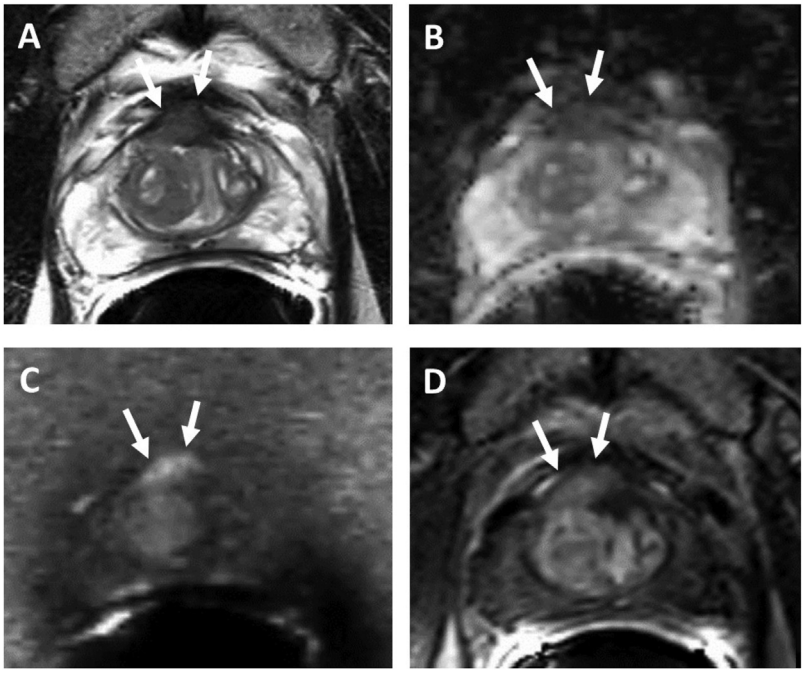

Fig. 4 – Prostate cancer appearing to involve the anterior fibromuscular stroma and thus scored using transition zone criteria. A 68-yr-old man with PSA 4.1 ng/ml and Gleason score 3 + 4 prostate cancer confirmed on MRI-guided targeted biopsy. (A) Axial T2-weighted image shows a lenticular homogeneous moderately T2 hypointense nodule (arrows) appearing to involve the anterior fibromuscular stroma with extraprostatic extension. (B) ADC map image shows focal hypointense signal corresponding to (A) (arrows). (C) Diffusion-weighted image (*b* = 2000) shows a markedly hyperintense signal (arrows) corresponding to (A) and (B). (D) Early dynamic contrast enhanced image shows avid enhancement within the anterior lesion (arrows). T2W MRI PI-RADS = 5, DW MRI PI-RADS = 5, DCE MRI PI-RADS = positive, PI-RADS assessment category = 5. ADC = apparent diffusion coefficient; DCE = dynamic contrast enhanced; DW = diffusion weighted; MRI = magnetic resonance imaging; PI-RADS = Prostate Imaging Reporting and Data System; PSA = prostate-specific antigen; T2W = T2 weighted.

3.2. *Evaluation of the TZ*

BPH is a histologic diagnosis showing glandular and stromal hyperplasia, and it manifests as a varying number of hyperplastic nodules and intervening tissue in the TZ in almost all men undergoing MRI for the assessment of PCa. Often, it is challenging on MRI to determine which, if any, findings in such a background should be scored and assigned a PI-RADS assessment category. PI-RADS v2.1 advises that the shape and margin features of TZ findings should be assessed in at least two planes on T2W MRI using the following criteria.

3.2.1. *What to score in the TZ*

Focal lesions, nodules, or regions in the TZ with features known to be associated with malignancy on T2W or DWI and those that differ from the predominant imaging characteristics of the background should be scored. For example, a lesion/region between nodules with more restricted diffusion than the background or a nodule with clearly more restricted diffusion than the background (on high *b*-value images and ADC maps) should be scored. A focal lesion that is different from other (background) nodules in having obscured margins, lenticular shape, or invasive behavior on T2W images, even if without differing restricted diffusion compared with the background, should also be scored.

Other findings should not be scored. For example, if there is restricted diffusion in multiple similar-appearing nodules scattered throughout the TZ, thus making restricted diffusion a feature of the background, these should not be scored.

3.2.2. *How to score in the TZ*

The T2W score is the dominant factor that determines the PI-RADS assessment category in the TZ, and a T2W score of 1 indicates a normal appearance of the TZ. In PI-RADS v2, typical BPH nodules (round, circumscribed, and completely or almost completely encapsulated on T2W) were assigned a T2W score of 2, and thus a PI-RADS assessment category of 2. However, since MRI findings of age-related BPH are present in the TZ in almost all men undergoing prostate mpMRI for the assessment of csPCa [22], and typical BPH nodules are highly unlikely to harbor csPCa [23], findings of BPH alone are considered a normal variant in PI-RADS v2.1 and should be assigned a T2W score of 1 (Fig. 5). These types of nodules do not have to be reported separately. Since every MRI examination should be assigned a PI-RADS assessment category of 1–5, when there are no findings with a PI-RADS assessment category of >1, the overall PI-RADS assessment category for the MRI examination should be reported as PI-RADS 1: clinically significant cancer is highly unlikely.

When circumscribed nodules in the TZ are incompletely or almost completely encapsulated, in PI-RADS v2.1, these atypical nodules are assigned a T2W score of 2.

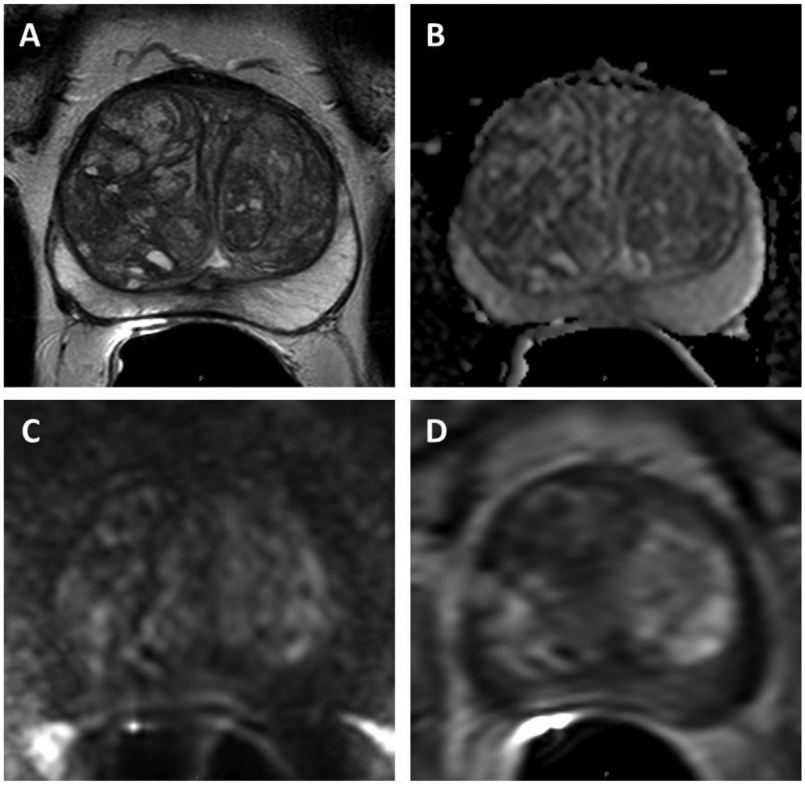

Fig. 5 – Transition zone with typical benign prostatic hyperplasia-related changes. (A) Axial T2-weighted image shows completely encapsulated "typical" nodules creating the "organized chaos" pattern. (B) ADC map image shows no focal lesion with low signal intensity below the background. (C) Diffusion-weighted image (*b* = 2000) shows no lesion with a markedly hyperintense signal above the background. (D) Early dynamic contrast enhanced image shows avid enhancement within the typical BPH nodules. T2W MRI PI-RADS = 1, DW MRI PI-RADS = 1, DCE MRI PI-RADS = negative, PI-RADS assessment category = 1. ADC = apparent diffusion coefficient; BPH = benign prostatic hyperplasia; DCE = dynamic contrast enhanced; DW = diffusion weighted; MRI = magnetic resonance imaging; PI-RADS = Prostate Imaging Reporting and Data System; T2W = T2 weighted.

Although the T2W score is the dominant factor that determines the PI-RADS assessment category in the TZ, restricted diffusion is also a feature of malignancy. In PI-RADS v2, DWI had no formal role in the differentiation of lesions in the TZ receiving PI-RADS assessment categories of 2 versus 3. However, occasionally, atypical nodules in the TZ may contain cancer, and DWI may be helpful in identifying them. In order to reflect the increased likelihood of PCa associated with high DWI scores in atypical TZ nodules, in PI-RADS v2.1, DWI features have been incorporated into scoring and determination of PI-RADS assessment categories for atypical TZ nodules. Thus, atypical TZ nodules (a T2W score of 2) are upgraded to PI-RADS assessment category 3 if they have a DWI score of $\geq$4 (ie, with markedly restricted diffusion; Fig. 6).

Mildly/moderately restricted diffusion is commonly encountered in mostly encapsulated and unencapsulated lesions in the TZ. Such lesions may represent areas of stromal hyperplasia and should not be upgraded on the basis of mildly/moderately restricted diffusion. Therefore, findings with a T2W score of 1 or 2 should not be upgraded to a PI-RADS assessment category of 2 or 3, respectively, based on a DWI score of 3 (ie, mildly/moderately restricted diffusion; Figs. 7 and 8).

In PI-RADS v2.1, the scoring of T2W for the TZ is modified as follows:

1: A normal appearing TZ (rare) or a round, completely encapsulated nodule ("typical nodule")
2: A mostly encapsulated nodule or a homogeneous circumscribed nodule without encapsulation ("atypical nodule") or a homogeneous mildly hypointense area between nodules
3: No change from PI-RADS v2 (heterogeneous signal intensity with obscured margins, including others that do not qualify as 2, 4, or 5)
4: No change from PI-RADS v2 (lenticular or noncircumscribed, homogeneous, moderately hypointense, and $<$1.5 cm in the greatest dimension)
5: No change from PI-RADS v2 (same as 4, but $\geq$1.5 cm in the greatest dimension or definite extraprostatic extension/invasive behavior).

Modification of the overall scoring schema for the TZ is shown in Table 1.

3.3. *Revision of the criteria for DWI scores 2 and 3*

PI-RADS v2 had problematic definitions for scores 2 and 3 for DWI. Score 2 on DWI included indistinct hypointense lesions on ADC. However, such lesions also commonly have a corresponding indistinct hyperintense appearance on high *b*-value DWI. Moreover, the meaning of the term "indistinct"

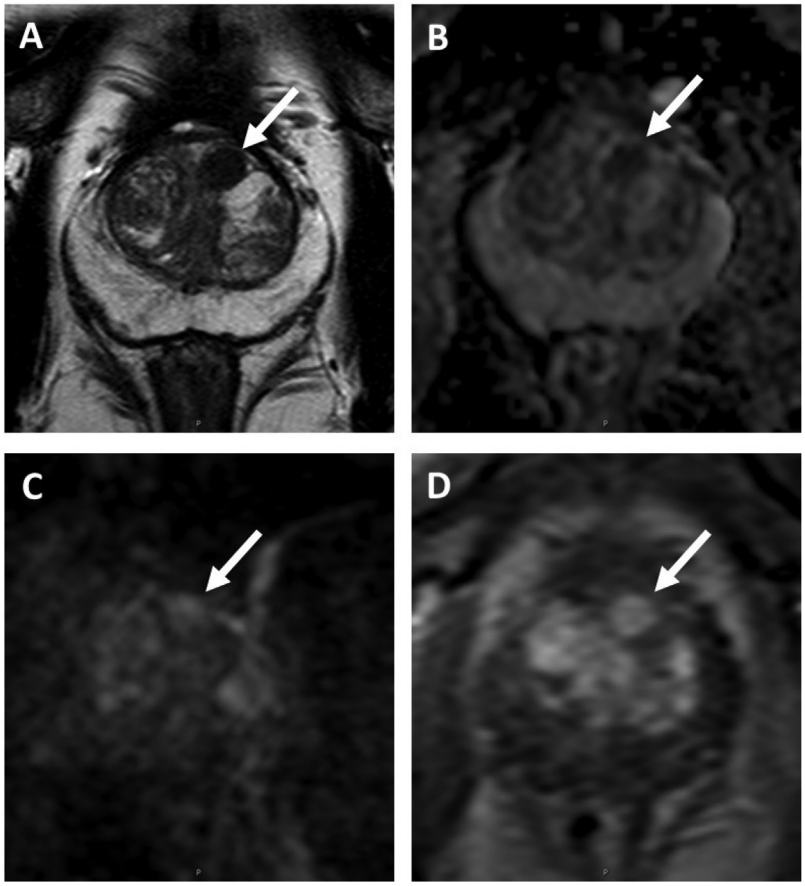

Fig. 6 – Transition zone with an atypical nodule. (A) Axial T2-weighted image shows a homogeneous T2 hypointense mostly encapsulated nodule (arrow). (B) ADC map image shows a focal lesion with a markedly hypointense signal below the background corresponding to the lesion seen in (A) (arrow). (C) Diffusion-weighted image (*b* = 1500) shows a focal lesion with a markedly hyperintense signal above the background (arrow) corresponding to the lesion seen in (A) and (B). (D) Early dynamic contrast enhanced image shows avid enhancement within the nodule (arrow). T2W MRI PI-RADS = 2, DW MRI PI-RADS = 4, DCE MRI PI-RADS = positive, PI-RADS assessment category = 3. ADC = apparent diffusion coefficient; DCE = dynamic contrast enhanced; DW = diffusion weighted; MRI = magnetic resonance imaging; PI-RADS = Prostate Imaging Reporting and Data System; T2W = T2 weighted.

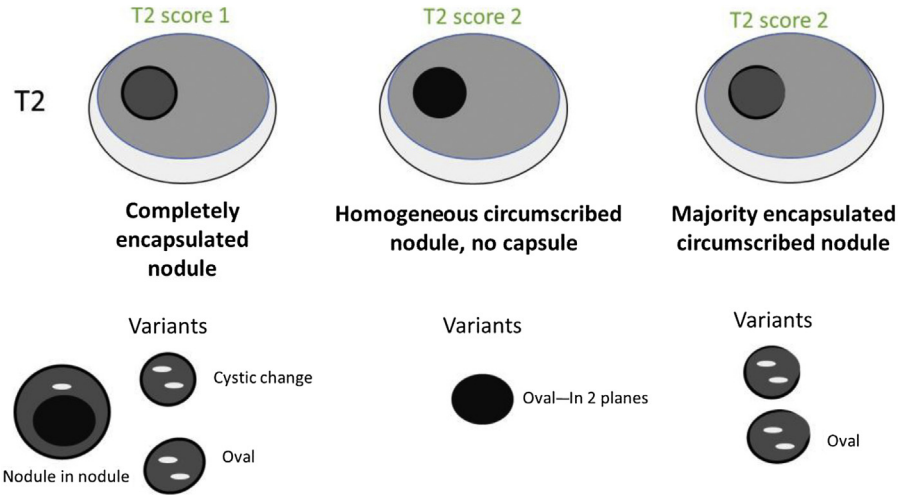

Fig. 7 – Schematic diagram of features of nodules in the TZ and their corresponding scores. Assessment of nodule shape and margins should be done in at least two planes. Oval or spherical shape and cystic change are acceptable features within nodules. TZ = transition zone.

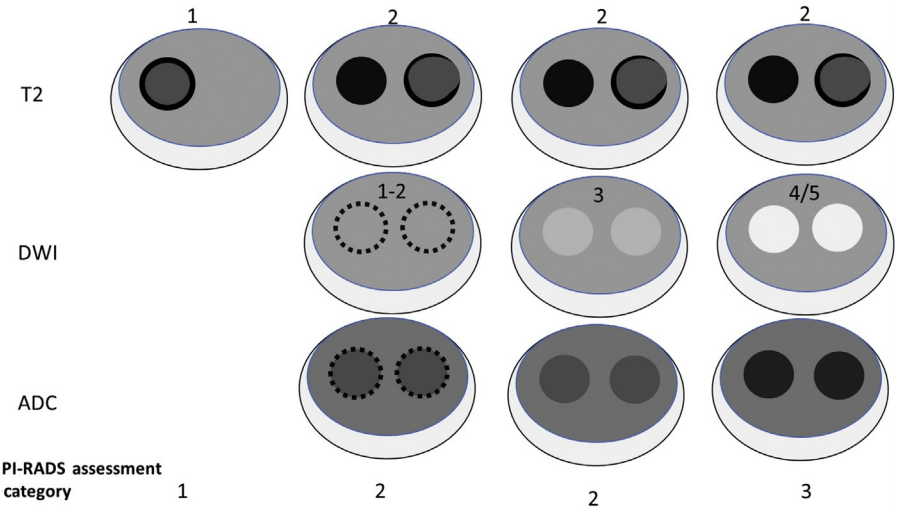

Fig. 8 – Schematic diagram of PI-RADS v2.1 scoring for TZ that incorporates DWI for the determination of assessment category for a partially encapsulated or circumscribed, uncapsulated nodule with clearly restricted diffusion (DWI score 4 or 5) is scored a 3 (dotted lines indicate the region of a near isointense lesion where the borders are indistinct or difficult to define because of the near isointensity). ADC = apparent diffusion coefficient; DWI = diffusion-weighted imaging; PI-RADS v2.1 = Prostate Imaging Reporting and Data System version 2.1; TZ = transition zone.

Table 1 – PI-RADS v2.1 assessment for TZ

T2	DWI	DCE	Overall
1	Any	Any	1
2	≤3	Any	2
	≥4	Any	3
3	≤4	Any	3
	5	Any	4
4	Any	Any	4
5	Any	Any	5

DCE = dynamic contrast enhanced; DWI = diffusion-weighted imaging; PI-RADS v2.1 = Prostate Imaging Reporting and Data System version 2.1; TZ = transition zone.

in the definition for DWI score 2, in comparison with the term "focal" in the criteria for DWI scores 3–5, was unclear. For DWI score 3, PI-RADS v2 definition was "focal mildly/moderately hypointense on ADC and isointense/mildly hyperintense on high b-value DWI," whereas for DWI score 4, the definition was "focal markedly hypointense on ADC and markedly hyperintense on high b-value DWI; <1.5 cm in greatest dimension." These criteria suggested that a lesion could be markedly positive on both ADC and high *b*-value DWI, but not on just one of the image sets, leading to uncertainty and variable interpretation regarding DWI scores 3 and 4.

For PI-RADS v2.1, scoring of DWI in all zones is revised as follows:

1: No change from PI-RADS v2
2: Linear/wedge-shaped hypointense on ADC and/or linear/wedge-shaped hyperintense on high *b*-value DWI
3: Focal (discrete and different from the background) hypointense on ADC and/or focal hyperintense on high *b*-value DWI; may be markedly hypointense on ADC or markedly hyperintense on high *b*-value DWI, but not both
4: No change from PI-RADS v2
5: No change from PI-RADS v2

In the PI-RADS v2.1 document, under "caveats for DWI", the term "marked" is defined as "a more pronounced signal change than any other focus in the same zone." These changes provide a more detailed definition for DWI score 3 and should reduce overcalling indeterminate lesions as category 4.

3.4. Clarification of the distinction between positive and negative enhancement on DCE MRI

In PI-RADS v2, the features that constituted a negative DCE score and assessment of widespread multifocal enhancement are unclear.

In PI-RADS v2.1, the criteria for a *positive* score on DCE are unchanged for PI-RADS v2: "focal, and; earlier than or contemporaneously with enhancement of adjacent normal prostatic tissues, and; corresponds to suspicious finding on T2W and/or DWI".

However, the criteria for a *negative* score on DCE in PI-RADS v2.1 have been modified: "no early or contemporaneous enhancement; or diffuse multifocal enhancement NOT corresponding to a focal finding on T2W and/or DWI."

It is anticipated that this change will decrease inter-reader variation in DCE MRI interpretations and reduce overcalls.

4. Role of DCE MRI

In PI-RADS v2, DCE MRI was a required component of mpMRI examinations undertaken for the detection of csPCa [4], although it had a very limited role and was used only when positive to elevate a finding in the PZ with a T2W score of 3–4. It did not have any formal role in scoring or

assessment category of findings in the TZ. However, experience has shown that, in some instances, DCE may assist in the detection of csPCa in both the PZ and the TZ [11,12], and in clinical practice, some have viewed DCE as a "safety-net" or "back-up" sequence, especially when DWI is degraded by artifacts or inadequate SNR.

Given the limited role of DCE, there is growing interest in performing prostate MRI without DCE, a procedure termed "biparametric MRI" (bpMRI). A number of recent studies have reported data that support the value of bpMRI for the detection of csPCa in biopsy-naïve men [24–28] and those with a prior negative biopsy [29].

The PI-RADS Steering Committee supports continued research concerning the performance of bpMRI in various clinical scenarios and acknowledges the potential benefits, including (1) elimination of adverse events and gadolinium retention that have been associated with some gadolinium-based contrast agents, (2) shortened examination time, and (3) reduced costs, possibly resulting in increased accessibility and utilization of MRI for biopsy-naïve men with suspected PCa.

However, the PI-RADS Steering Committee also has a concern. In some studies, DCE MRI has been reported to improve the sensitivity of prostate mpMRI [11,12,29]. Although most of the bpMRI studies are prospective, they were performed using different methodologies at single institutions with only one or two readers. It is possible that the performance of bpMRI will be degraded in multi-institutional clinical trials with multiple readers, and while further research is required, at this time there may be an increase in the frequency of missed csPCa cases if bpMRI were to receive widespread clinical adoption. Furthermore, as described above, DCE in practice has been a "safety-net" or "back-up" sequence, especially when either T2W or DWI is degraded by artifacts or inadequate SNR, a situation that is not uncommon on some MRI scanners when performing prostate MRI without an endorectal coil. Thus, it is important to perform further research, before DCE is deemed unnecessary for assessment of treatment-naïve prostate patients. DCE remains essential in the assessment of local recurrence following prior treatment, a setting in which current PI-RADS assessment criteria do not apply.

The PI-RADS Steering Committee encourages multicenter prospective studies, employing multiple readers and addressing relative biopsy yields of csPCa and indolent PCa of mpMRI-directed biopsy prompted by both approaches, with transrectal ultrasound (TRUS)-guided biopsy comparisons to see whether the documented advantages of mpMRI-directed biopsy are retained by bpMRI [28,30].

For now, the committee suggests that bpMRI be reserved for select clinical indications and makes the following recommendations regarding when mpMRI is preferred over bpMRI usage:

1. Multiparametric MRI is still preferred in men where the balance between under- and overdiagnosis favors the clinical priority of not missing any significant cancer. These patients include those with prior negative biopsies with unexplained raised prostate-specific antigen (PSA) values, and those in active surveillance who are being evaluated for fast PSA doubling times or changing clinical/pathologic status.
2. For men who have previously undergone a bpMRI examination that did not show findings suspicious for csPCa and those who remain at persistent suspicion of harboring disease, the clinical priority for subsequent MRI scans is to not miss csPCa; thus, the preferred reimaging option is mpMRI.
3. Prior prostate interventions (TRUS/transrectal resection of the prostate/BPH therapy, radiotherapy, focal therapy, or embolization) and drug/hormonal therapies (testosterone, 5-alpha reductase, etc.) that are known to change prostate morphology should be evaluated with mpMRI, at a suitable time after the surgical intervention, for disease detection and localization.
4. Biopsy-naïve men with a strong family history, known genetic predispositions, elevated urinary genomic scores, and higher than average risk calculator scores for csPCa should have mpMRI.

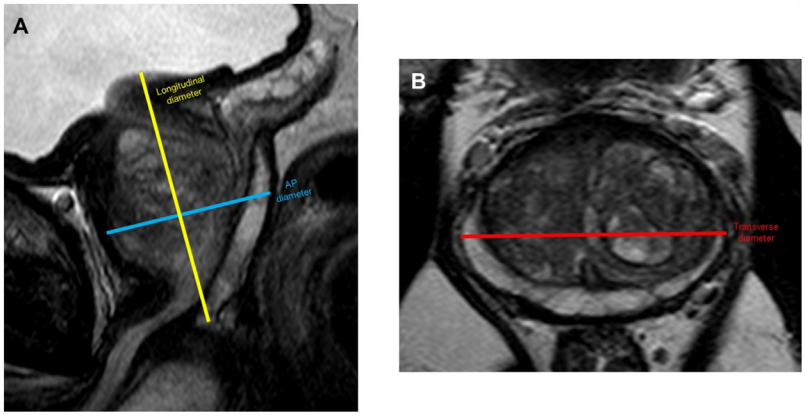

Fig. 9 – Suggested measurements for ellipsoid formula when calculating prostate volume at MRI. (A) Maximum longitudinal diameter and maximum AP diameter should be measured on midsagittal T2W MRI, whereas (B) maximum transverse diameter should be measured on axial T2W MRI. AP = anteroposterior; MRI = magnetic resonance imaging; T2W = T2 weighted.

5. Men with a hip implant or other considerations that can be expected to yield degraded DWI should have mpMRI.

5. Implications of bpMRI for PI-RADS assessment categories

When bpMRI is performed and DCE data are not obtained, TZ assessment remains unchanged. The PI-RADS assessment category for a finding in the PZ remains primarily based on the DWI score, and the lesions that receive a score of 3 on DWI will not be upgraded. The proportion of men with PI-RADS assessment category 3 will likely increase and the proportion with PI-RADS assessment category 4 will reduce, and in so doing change the likelihood of csPCa in these PI-RADS categories, which will require additional documentation and subsequently pathway modifications for both biopsy-naïve men and men with prior negative biopsy [31].

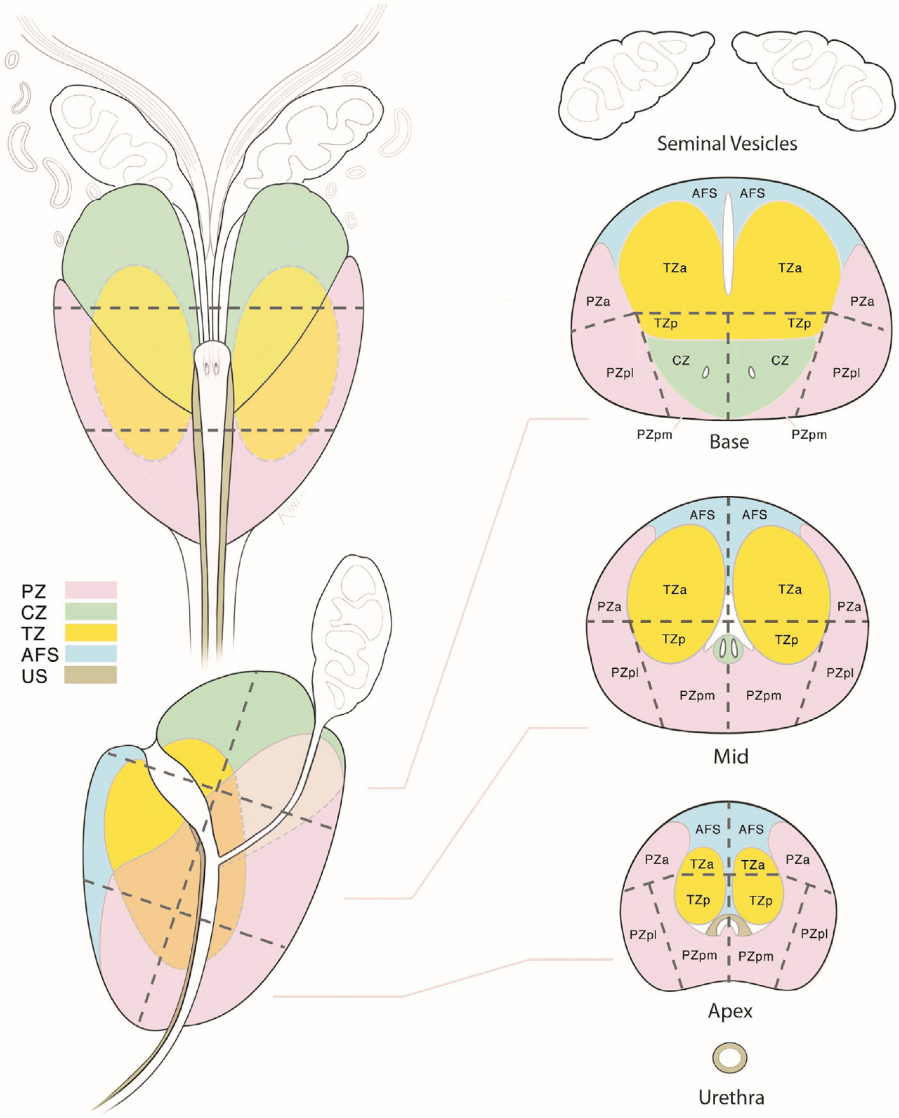

Fig. 10 – Sector map diagram for version 2.1: the segmentation model used in PI-RADS v2.1 employs 38 sectors/regions for the prostate, two for the seminal vesicles, and one for the membranous urethra (total 41). Each of the right and left peripheral zones (PZs) at the prostate base, midgland, and apex is subdivided into three sections: anterior (a), posterior medial (pm), and posterior lateral (pl). Each of the right and left transition zones (TZs) at the prostate base, midgland, and apex is subdivided into two sections: anterior (a) and posterior (p). The anterior fibromuscular stroma is divided into right and left sections at the prostate base, midgland, and apex. The seminal vesicles are divided into right and left sections. The sector map illustrates an idealized prostate. Since the prior version, in addition to two new sectors at the base, there have been adjustments to the location of ejaculatory ducts, angulation of the proximal urethra, and overall proportions of the gland to match between the coronal, sagittal, and axial images. In patients and their corresponding MRI images, most prostates have anatomical components that are enlarged or atrophied, and the PZ may be obscured by an enlarged TZ, and CZ may not be easily identifiable. In such instances, a diagram is used as an approximation of the gland and a sector map can be marked to indicate the location of the findings in addition to the written report. AFS = anterior fibromuscular stroma; CZ = central zone; MRI = magnetic resonance imaging; PI-RADS v2.1 = Prostate Imaging Reporting and Data System version 2.1. *Note.* The prostate sector diagram was modified by David A. Rini, MFA, CMI, FAMI, Associate Professor in the Department of Art as Applied to Medicine at the Johns Hopkins University, based on previously published figures by Villers et al. (Curr Opin Urol 2009;19:274–82) and Dickinson et al. (Eur Urol 2011;59:477–94) with anatomical correlation to the normal histology of the prostate by McNeal JE (Am J Surg Pathol 1988 Aug;12:619–33).

6. Clarification in measurement of the prostate volume

PI-RADS v2 recommended to routinely report the prostate volume based on MRI, using manual or automated segmentation or calculations using ellipsoid formulation ([maximum anteroposterior {AP} diameter] × [maximum transverse diameter] × [maximum longitudinal diameter] × 0.52). Recent studies have demonstrated a need for reliable prostate volume assessments on MRI when the MRI volume is used to derive serum PSA density (reported in ng/ml^2) measured using the following formula: serum PSA/prostate volume [32,33]. PI-RADS v2.1 aims to ensure that a uniform approach is used to calculate prostate volume when using the ellipsoid formulation. PI-RADS v2.1 recommends that the maximum AP and longitudinal diameters are placed on the midsagittal T2W image, while the maximum transverse diameter is placed on the axial T2W image (Fig. 9).

7. Revisions in the sector map

The sector map of PI-RADS v2 document has been in use since its release. The segmentation model used in PI-RADS v2 was adapted from a European consensus meeting and the ESUR Prostate MRI guidelines 2012 [34]. The map illustrated an idealized "normal prostate" and employed 39 sectors/regions: 36 for the prostate, two for the seminal vesicles, and one for the membranous urethra. In PI-RADS v2.1, the revised sector map contains two additional sectors in the base PZ: right and left posterior PZ medial, as depicted in Fig. 10. With this revision, there are now 38 prostate sectors, plus two for the seminal vesicles and one for the membranous urethra, amounting to a total 41 sectors. In addition, some other minor improvements were made in order to better match age-related anatomy (eg, angulated urethra) and the image acquisition planes.

8. Summary

In the few years since its publication, PI-RADS v2 has achieved important goals for standardization of image acquisition and interpretation of prostate MRI, with worldwide acceptance in academic and community settings. Furthermore, PI-RADS v2 has been incorporated into various PCa guidelines from professional medical organizations and used in the majority of research publications from all medical specialties that assess prostate mpMRI. Experience using PI-RADS v2 has identified a number of ambiguities and limitations, some of which have been documented in the literature with potential solutions offered. The PI-RADS Steering Committee has considered such issues and addressed them in PI-RADS v2.1. It is anticipated that the adoption of these PI-RADS v2.1 modifications will improve inter-reader variability and simplify PI-RADS assessment of prostate MRI even further. As previously indicated, continued evolution and development of PI-RADS into a version 3 is anticipated as further clinical experience and investigative data are accrued. Research on the value and limitations on all components of PI-RADS v2.1 is strongly encouraged.

Author contributions: Baris Turkbey had full access to all the data in the study and takes responsibility for the integrity of the data and the accuracy of the data analysis.

Study concept and design: All authors.
Acquisition of data: None.
Analysis and interpretation of data: None.
Drafting of the manuscript: Turkbey, Rosenkrantz.
Critical revision of the manuscript for important intellectual content: All authors.
Statistical analysis: None.
Obtaining funding: None.
Administrative, technical, or material support: None.
Supervision: Weinreb, Barentsz.
Other: None.

Financial disclosures: Baris Turkbey certifies that all conflicts of interest, including specific financial interests and relationships and affiliations relevant to the subject matter or materials discussed in the manuscript (eg, employment/affiliation, grants or funding, consultancies, honoraria, stock ownership or options, expert testimony, royalties, or patents filed, received, or pending), are the following: Baris Turkbey: no disclosure. Andrew B. Rosenkrantz: Royalties from Thieme Medical Publishers. Masoom A. Haider: no disclosure. Anwar R. Padhani: no disclosure. Geert Villeirs: no disclosure. Katarzyna J. Macura: no disclosures relevant to the submitted work within last 12 months; Research Grant Support: GlaxoSmithKline, Profound Medical, Siemens Healthineers; Royalties, Author: Elsevier. Clare M. Tempany: NIH funding-P41 EB 015898, R25 NCI CA089017; Industry clinical trial support: InSightec Inc, Gilead Sciences; Consulting Honoraria: Profound Medical. Peter L. Choyke: no disclosure. Francois Cornud: no disclosure. Daniel J. Margolis: receives a consideration for ad-hoc consulting to Blue Earth Diagnostics. Harriet C. Thoeny: no disclosure. Sadhna Verma: no disclosure. Jelle Barentsz: no disclosure. Jeffrey C. Weinreb: Medicolegal consultant for Bayer Healthcare Pharmaceuticals.

Funding/Support and role of the sponsor: None.

Acknowledgments: The authors would like to thank Mythreyi Chatfield and Lauren Hicks (American College of Radiology); Faina Shtern (AdMeTech Foundation); European Society of Urogenital Radiology (ESUR); external reviewers: Rajan Gupta (Duke University, USA), Steve Raman (UCLA, USA), Aytekin Oto (University of Chicago, USA), Daniel Costa (University of Texas Southwestern Medical Center, USA), Andrei Purysko (Cleveland Clinic, USA), Valeria Panebianco (Sapienza University of Rome, Italy), Tristan Barrett (University of Cambridge School of Clinical Medicine, UK), Phillipe Puech (CHU Lille, University of Lille, France), Vibeke Løgager (University of Copenhagen, Denmark), Bernd Hamm (Charité, Universitätsmedizin Berlin, Germany), Samir Taneja (NYU, USA), Peter Pinto (National Cancer Institute, USA), Leonard Marks (UCLA, USA), and Preston Sprenkle (Yale School of Medicine, USA); and David A. Rini (Johns Hopkins University) for sector diagram.

References

[1] Renard-Penna R, Rouviere O, Puech P, et al. Current practice and access to prostate MR imaging in France. Diagn Interv Imaging 2016;97:1125–9.
[2] Oberlin DT, Casalino DD, Miller FH, Meeks JJ. Dramatic increase in the utilization of multiparametric magnetic resonance imaging for detection and management of prostate cancer. Abdom Radiol 2017;42:1255–8.

[3] Gupta RT, Spilseth B, Froemming AT. How and why a generation of radiologists must be trained to accurately interpret prostate mpMRI. Abdom Radiol 2016;41:803–4.
[4] Weinreb JC, Barentsz JO, Choyke PL, et al. PI-RADS Prostate Imaging – Reporting and Data System: 2015, version 2. Eur Urol 2016;69:16–40.
[5] Spilseth BD, Patel GS, Taneja NU, Margolis SS, Rosenkrantz DJ. A comparison of radiologists' and urologists' opinions regarding prostate MRI reporting: results from a survey of specialty societies. Am J Roentgenol 2018;210:101–7.
[6] Purysko AS, Bittencourt LK, Bullen JA, Mostardeiro TR, Herts BR, Klein EA. Accuracy and interobserver agreement for Prostate Imaging Reporting and Data System, version 2, for the characterization of lesions identified on multiparametric MRI of the prostate. AJR Am J Roentgenol 2017;209:339–49.
[7] Seo JW, Shin SJ, Taik Oh Y, et al. PI-RADS version 2: detection of clinically significant cancer in patients with biopsy Gleason score 6 prostate cancer. AJR Am J Roentgenol 2017;209:W1–9.
[8] Mehralivand S, Bednarova S, Shih JH, et al. Prospective evaluation of Prostate Imaging Reporting and Data System, version 2 using the International Society of Urological Pathology Prostate Cancer Grade Group system. J Urol 2017;198:583–90.
[9] Woo S, Suh CH, Kim SY, Cho JY, Kim SH. Diagnostic performance of Prostate Imaging Reporting and Data System version 2 for detection of prostate cancer: a systematic review and diagnostic meta-analysis. Eur Urol 2017;72:177–88.
[10] Padhani AR, Weinreb J, Rosenkrantz AB, Villeirs G, Turkbey B, Barentsz J. Prostate Imaging-Reporting and Data System Steering Committee: PI-RADS v2 status update and future directions. Eur Urol 2019;75:385–96.
[11] Greer MD, Shih JH, Lay N, et al. Validation of the dominant sequence paradigm and role of dynamic contrast-enhanced imaging in PI-RADS version 2. Radiology 2017;285:859–69.
[12] Rosenkrantz AB, Babb JS, Taneja SS, Ream JM. Proposed adjustments to PI-RADS version 2 decision rules: impact on prostate cancer detection. Radiology 2017;283:119–29.
[13] Greer MD, Brown AM, Shih JH, et al. Accuracy and agreement of PIRADSv2 for prostate cancer mpMRI: a multireader study. J Magn Reson Imaging 2017;45:579–85.
[14] Rosenkrantz AB, Ginocchio LA, Cornfeld D, et al. Interobserver reproducibility of the PI-RADS version 2 lexicon: a multicenter study of six experienced prostate radiologists. Radiology 2016;280:793–804.
[15] Rosenkrantz AB, Oto A, Turkbey B, Westphalen AC. Prostate Imaging Reporting and Data System (PI-RADS), version 2: a critical look. AJR Am J Roentgenol 2016;206:1179–83.
[16] Rosenkrantz AB, Padhani AR, Chenevert TL, et al. Body diffusion kurtosis imaging: basic principles, applications, and considerations for clinical practice. J Magn Reson Imaging 2015;42:1190–202.
[17] Ream JM, Doshi AM, Dunst D, et al. Dynamic contrast-enhanced MRI of the prostate: an intraindividual assessment of the effect of temporal resolution on qualitative detection and quantitative analysis of histopathologically proven prostate cancer. J Magn Reson Imaging 2017;45:1464–75.
[18] Othman AE, Falkner F, Weiss J, et al. Effect of temporal resolution on diagnostic performance of dynamic contrast-enhanced magnetic resonance imaging of the prostate. Invest Radiol 2016;51:290–6.
[19] Vargas HA, Akin O, Franiel T, et al. Normal central zone of the prostate and central zone involvement by prostate cancer: clinical and MR imaging implications. Radiology 2012;262:894–902.
[20] Ward E, Baad M, Peng Y, et al. Multi-parametric MR imaging of the anterior fibromuscular stroma and its differentiation from prostate cancer. Abdom Radiol (NY) 2017;42:926–34.
[21] Bouye S, Potiron E, Puech P, Leroy X, Lemaitre L, Villers A. Transition zone and anterior stromal prostate cancers: zone of origin and intraprostatic patterns of spread at histopathology. Prostate 2009;69:105–13.
[22] Turkbey B, Huang R, Vourganti S, et al. Age-related changes in prostate zonal volumes as measured by high-resolution magnetic resonance imaging (MRI): a cross-sectional study in over 500 patients. BJU Int 2012;110:1642–7.
[23] Chesnais AL, Niaf E, Bratan F, et al. Differentiation of transitional zone prostate cancer from benign hyperplasia nodules: evaluation of discriminant criteria at multiparametric MRI. Clin Radiol 2013;68:e323–30.
[24] Lars Boesen M, Nørgaard N, Løgager V, et al. Assessment of the diagnostic accuracy of biparametric magnetic resonance imaging for prostate cancer in biopsy-naive men: the Biparametric MRI for Detection of Prostate Cancer (BIDOC) study. JAMA Netw 2018;1:e180219.
[25] Jambor I, Bostrom PJ, Taimen P, et al. Novel biparametric MRI and targeted biopsy improves risk stratification in men with a clinical suspicion of prostate cancer (IMPROD trial). J Magn Reson Imaging 2017;46:1089–95.
[26] Cuocolo R, Stanzione A, Rusconi G, et al. PSA-density does not improve bi-parametric prostate MR detection of prostate cancer in a biopsy naive patient population. Eur J Radiol 2018;104:64–70.
[27] Weiss J, Martirosian P, Notohamiprodjo M, et al. Implementation of a 5-minute magnetic resonance imaging screening protocol for prostate cancer in men with elevated prostate-specific antigen before biopsy. Invest Radiol 2018;53:186–90.
[28] Barth BK, De Visschere PJL, Cornelius A, et al. Detection of clinically significant prostate cancer: short dual-pulse sequence versus standard multiparametric MR imaging—a multireader study. Radiology 2017;284:725–36.
[29] Krishna S, McInnes M, Lim C, et al. Comparison of Prostate Imaging Reporting and Data System versions 1 and 2 for the detection of peripheral zone Gleason score 3 + 4 = 7 cancers. AJR Am J Roentgenol 2017;209:W365–73.
[30] Kuhl CK, Bruhn R, Kramer N, Nebelung S, Heidenreich A, Schrading S. Abbreviated biparametric prostate MR imaging in men with elevated prostate-specific antigen. Radiology 2017;285:493–505.
[31] Junker D, Steinkohl F, Fritz V, et al. Comparison of multiparametric and biparametric MRI of the prostate: are gadolinium-based contrast agents needed for routine examinations? World J Urol 2019;37:691–9.
[32] Lee SJ, Oh YT, Jung DC, Cho NH, Choi YD, Park SY. Combined analysis of biparametric MRI and prostate-specific antigen density: role in the prebiopsy diagnosis of Gleason score 7 or greater prostate cancer. AJR Am J Roentgenol 2018;211:W166–72.
[33] Mehralivand S, Shih JH, Rais-Bahrami S, et al. A magnetic resonance imaging-based prediction model for prostate biopsy risk stratification. JAMA Oncol 2018;4:678–85.
[34] Barentsz JO, Richenberg J, Clements R, et al. ESUR prostate MR guidelines 2012. Eur Radiol 2012;22:746–57.